Asymmetric Hydrogenation of Enamides with Rh-BisP* and Rh-MiniPHOS Catalysts. Scope, Limitations, and Mechanism

Ilya D. Gridnev,* Masaya Yasutake, Natsuka Higashi, and Tsuneo Imamoto*

Contribution from the Department of Chemistry, Faculty of Science, Chiba University, Inage-ku, Chiba 263-8522, Japan

Received January 18, 2001

Abstract: The asymmetric hydrogenation of aryl- and alkyl-substituted enamides catalyzed by Rh-BisP* complex affords optically active amides with very high ee values. The Rh-MiniPHOS catalyst gives somewhat less satisfactory results. Hydrogenation of the aryl-substituted enamides with (*S*,*S*)-BisP*-Rh catalyst gives *R*-amides, whereas the *t*-Bu- and 1-adamantyl-substituted enamides give *S*-products with 99% ee. Reaction of [Rh(BisP*)-(CD$_3$OD)$_2$]BF$_4$ (**11**) with CH$_2$=C(C$_6$H$_5$)NHCOCH$_3$ (**5**) gives two diastereomers of the catalyst−substrate complex (**12a,b**), which interconvert reversibly by both intra- and intermolecular pathways as shown by EXSY data. Only one isomer in equilibrium with solvate complex **11** was detected for each of the catalyst−substrate complexes **17** and **18** obtained from CH$_2$=C(*t*-Bu)NHCOCH$_3$ (**6**) or CH$_2$=C(1-adamantyl)NHCOCH$_3$ (**7**). Hydrogenation of these equilibrium mixtures at −100 °C gave monohydride intermediates **19** and **20**, respectively. In these monohydrides the Rh atom is bound to the β-carbon. A new effect of the significant decrease of ee was found for the asymmetric hydrogenation of CH$_2$=C(C$_6$H$_4$OCH$_3$-*o*)NHCOCH$_3$ (**21**), when H$_2$ was substituted for HD or D$_2$.

Introduction

Optically active 1-arylalkylamines are useful compounds from many points of view.[1] The possibility of producing chiral amides directly by asymmetric hydrogenation of enamides was recognized in 1975 by Kagan,[2] who achieved 90% optical yields in some hydrogenations catalyzed by Rh(I)-DIOP.[2,3] For a long time comparable results could not be obtained with other diphosphine ligands.[4] Note, however, that a successful application of Ru-catalyzed asymmetric hydrogenation for the synthesis of isoquinoline alkaloids was reported by Noyori et al.[5] The breakthrough was achieved with the introduction of BPE and DuPHOS ligands, which gave up to 98.5% enantioselectivity in Rh-catalyzed asymmetric hydrogenations of enamides.[6] Later, rhodium complexes of such ligands as BICP,[7] H$_8$-BINAM,[8] TRAP,[9] Binaphane,[10] and modified DIOP[11,12] were also found to be effective for similar hydrogenation. It was shown recently in our group that new structurally simple P-chirogenic diphosphines abbreviated as BisP*[13,14] and MiniPHOS[14−16] give Rh complexes, which are effective catalysts for the asymmetric hydrogenation of dehydroamino acids providing a wide series of unnatural amino acids with excellent ee values. Therefore,

we were prompted to examine the synthetic utility of these complexes in the asymmetric hydrogenation of enamides. Furthermore, a mechanistic study of asymmetric hydrogenation of methyl (*Z*)-α-acetamidocinnamate catalyzed by BisP*-Rh complex revealed some new aspects of the reaction pathway.[17] Most of the previous mechanistic studies in the field of Rh-catalyzed asymmetric hydrogenation have been done for dehydroamino acids.[18,19] In the usual explanations of the stereoselection mechanism in the catalytic asymmetric hydrogenations the carboxy group of a dehydroamino acid is regarded as an important stereoregulating factor.[18,20−23] In the structure of an enamide the carboxy group is absent, but the nature of the substituent at the α-position can be varied without losing the high degree of enantioselectivity. Therefore, a mechanistic study of catalytic asymmetric hydrogenation of enamides can provide new details of the structure of the intermediates and the mechanism of stereoselection in the Rh-catalyzed hydrogenations.
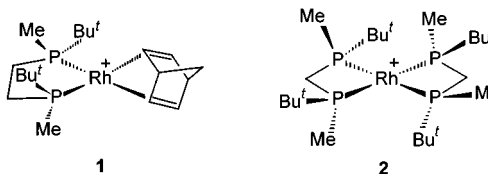
In this paper we report detailed studies of the scope and limitations of the asymmetric hydrogenation of enamides

(1) Nogradi, M. *Stereoselective Synthesis*, 2nd ed.; VCH: Weinheim, 1995.

(2) Kagan, H. B.; Langlois, N.; Dang, T. P. *J. Organomet. Chem.* **1975**, *90*, 353.

(3) Sinou, D.; Kagan, H. B. *J. Organomet. Chem.* **1976**, *114*, 325−337.

(4) Morimoto, T.; Chiba, M.; Achiwa, K. *Chem. Pharm. Bull.* **1992**, *40*, 2894−2896.

(5) Noyori, R.; Ohta, M.; Hisao, Y.; Kitamura, M.; Ohta, T.; Takaya, H. *J. Am. Chem. Soc.* **1986**, *108*, 7117−7119.

(6) Burk, M. J.; Wang, Y. M.; Lee, J. R. *J. Am. Chem. Soc.* **1996**, *118*, 5142−5143.

(7) Zhu, G.; Zhang, X. *J. Org. Chem.* **1998**, *63*, 9590−9593.

(8) Zhang, F.-Y.; Pai, C.-C.; Chan, A. S. C. *J. Am. Chem. Soc.* **1998**, *120*, 5808−5809.

(9) Kuwano, R.; Sato, K.; Kurokawa, T.; Karube, D.; Ito, Y. *J. Am. Chem. Soc.* **2000**, *122*, 7614−7615.

(10) Xiao, D.; Zhang, Z.; Zhang, X. *Org. Lett.* **1999**, *1*, 1679−1681.

(11) Li, W.; Zhang, X. *J. Org. Chem.* **2000**, *65*, 5871−5874.

(12) Yan, Y.; RajanBabu, T. V. *Org. Lett.* **2000**, 4137−4140.

(13) Imamoto, T.; Watanabe, J.; Wada, Y.; Masuda, H.; Yamada, H.; Tsuruta, H.; Matsukawa, S.; Yamaguchi, K. *J. Am. Chem. Soc.* **1998**, *120*, 1635−1636.
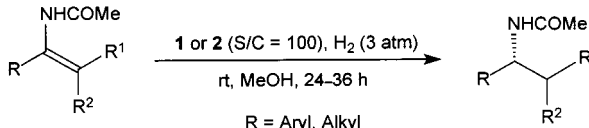
(14) Gridnev, I. D.; Yamanoi Y.; Higashi, N.; Tsuruta, H.; Yasutake, M.; Imamoto, T. *Adv. Synth., Catal.* **2001**, *343*, 118−136.

(15) Yamanoi, Y.; Imamoto, T. *J. Org. Chem.* **1999**, *64*, 2988−2989.

(16) Gridnev I. D.; Imamoto, T. *Organometallics* **2001**, *20*, 545−549.

(17) Gridnev, I. D.; Higashi, N.; Asakura, K.; Imamoto, T. *J. Am. Chem. Soc.* **2000**, *122*, 7183−7194.

(18) Brown, J. M. *Hydrogenation of Functionalized Carbon−Carbon Double Bonds*; Jacobsen, E. N., Pfaltz, A., Yamamoto, H., Eds.; Springer: Berlin, 1999; Vol. 1, pp 119−182.

Asymmetric Hydrogenation of Enamides

J. Am. Chem. Soc., Vol. 123, No. 22, 2001 5269

Table 1. Enantioselective Hydrogenation of Aryl- and Alkylenamides Catalyzed by *t*-Bu-BisP*and *t*-Bu-MiniPHOS[a]

entry	Ar	R^1, R^2	precatalyst	ee, %
1	C$_6$H$_5$	H, H	**1**	99 (*R*)
2	C$_6$H$_5$	H, H	**2**	66 (*R*)
3	2-CH$_3$OC$_6$H$_4$	H, H	**1**	50 (*R*)
4	2-CH$_3$OC$_6$H$_4$	H, H	**2**	47 (*R*)
5	3-CH$_3$OC$_6$H$_4$	H, H	**1**	97 (*R*)
6	3-CH$_3$OC$_6$H$_4$	H, H	**2**	87 (*R*)
7	4-CH$_3$OC$_6$H$_4$	H, H	**1**	96 (*R*)
8	4-CH$_3$OC$_6$H$_4$	H, H	**2**	86 (*R*)
9	2-ClC$_6$H$_4$	H, H	**1**	46 (*R*)
10	2-ClC$_6$H$_4$	H, H	**2**	16 (*R*)
11	3-ClC$_6$H$_4$	H, H	**1**	93 (*R*)
12	3-ClC$_6$H$_4$	H, H	**2**	71 (*R*)
13	4-ClC$_6$H$_4$	H, H	**1**	99 (*R*)
14	4-ClC$_6$H$_4$	H, H	**2**	88 (*R*)
15	3-CH$_3$OCOC$_6$H$_4$	H, H	**1**	99 (*R*)
16	3-CH$_3$OCOC$_6$H$_4$	H, H	**1*** [b]	97 (*S*)
17	C$_6$H$_5$	Me, Me	**1**	99 (*R*)
18	C$_6$H$_5$	Me, Me	**2**	98 (*R*)
19	*t*-Bu	H, H	**1**	99 (*S*)
20	1-Adamantyl	H, H	**1**	99 (*S*)
21	1-Adamantyl	H, H	**2**	99 (*S*)

[a] Reactions were carried out in MeOH at room temperature under an initial H$_2$ pressure of 3 atm and S/C = 100 for 24−36 h. The yields were quantitative. [b] **1*** is [Rh((*R,R*)-*t*-Bu-BisP*)]BF$_4$.

catalyzed by the rhodium complexes of *t*-Bu-BisP* (**1**) and *t*-Bu-MiniPHOS (**2**) as well as the mechanistic studies carried out for a wide range of substrates.[24]

Results and Discussion

Catalytic Hydrogenation of Enamides with Rh-BisP* and Rh-MiniPHOS Catalysts. The results of the catalytic asymmetric hydrogenation of enamides catalyzed by rhodium complexes of *t*-Bu-BisP* and *t*-Bu-MiniPHOS are summarized in Table 1. It should be noted that enantioselectivities approaching 100% have been achieved for a wide range of substrates (entries 1, 5, 7, 11, 13, 15, and 17−21). Almost no solvent dependence of the stereochemical purity was found (Table S1), and hence methanol was used throughout the further studies.

The BisP*-based catalyst **1** is optimal; it gave better results compared to **2** in all the studied cases. The *m*- and *p*-methoxy- and chloro-substituted phenylenamides gave high ee values (entries 5, 7, 11, and 13), but for their ortho-substituted analogues the optical yields were drastically decreased (entries 3, 4, 9, and 10). This result suggests that the absence of steric hindrance around the double bond of aromatic enamide is an important factor for the successful asymmetric hydrogenation.

Entry 16 demonstrates the applicability of the described method to the asymmetric synthesis of practically useful

Scheme 1
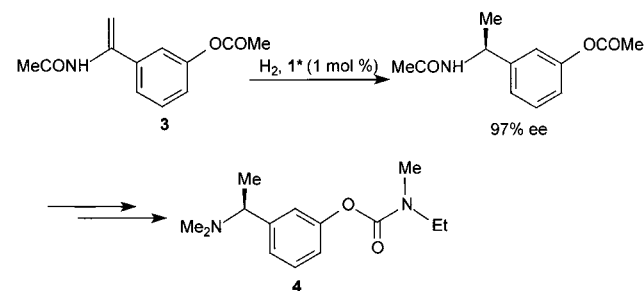
Scheme 2
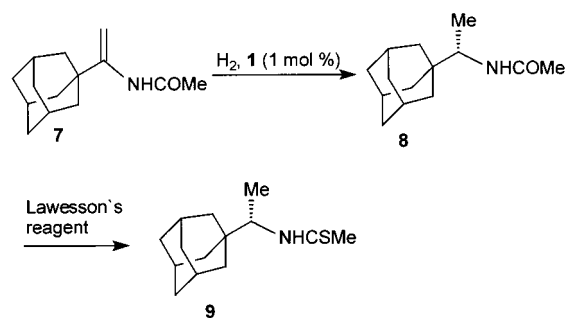
compounds. Thus, the successful asymmetric hydrogenation of 3-methoxy-substituted substrate **3** (entries 15 and 16) enables the effective introduction of an asymmetric center in the synthesis of the acetylcholinesterase inhibitor SDZ-ENA-713 (**4**) (Scheme 1).[25−29]

Particularly interesting is the dramatic difference in the sense of stereoselection observed for all the studied aryl-substiuted enamides (giving *R*-products) and the enamides containing bulky *tert*-butyl and 1-adamantyl groups (giving *S*-products with excellent ee values, entries 19−21). Burk et al. have reported a similar effect observed in asymmetric hydrogenation of 1-acetylamino-1-phenylethene (**5**), 1-acetylamino-1-*tert*-butylethene (**6**), and 1-acetylamino-1-(1-adamantyl)ethene (**7**) catalyzed by a DuPHOS-Rh complex.[6,30] We could not employ the previously reported sophisticated chromatographic conditions for the separation of the enantiomers of the adamantyl-substituted hydrogenation product (**8**).[30] The separation was achieved on HPLC using the UV detector adjusted for 210 nm, but the absolute configuration of our product could not be assigned at this stage, since the [α]$_D$ values have not been previously reported. The exact structure of **8**, obtained by the hydrogenation of **7** in the presence of **1**, was determined by converting it to thioamide **9**, the *S* absolute configuration of which was determined by the Flack parameter obtained in the single-crystal X-ray study (Scheme 2).

Thus, our data unequivocally indicate that the sense of enantioselection in the asymmetric hydrogenation of enamides stands in close correlation to the stereochemical environment of the double bond of the enamide, leading in extreme cases to the complete inversion of the sense of enantioselection. To

(19) Landis, C. R.; Hilfenhaus, P.; Feldgus, S. *J. Am. Chem. Soc.* **1999**, *121*, 8741−8754.

(20) Vineyard, B. D.; Knowles, W. S.; Sabacky, G. L.; Bachman, G. L.; Weinkauff, D. J. *J. Am. Chem. Soc.* **1977**, *99*, 5946−5952.

(21) Koenig, K. E.; Sabacky, M. J.; Bachman, G. L.; Christopfel, W. C.; Barnstorff, H. D.; Friedman, R. B.; Knowles, W. S.; Stults, B. R.; Vineyard, B. D.; Weinkauff, D. J. *Ann. N.Y. Acad. Sci.* **1980**, *333*, 16−22.

(22) Knowles, W. S. *Acc. Chem. Res.* **1983**, *16*, 106−112.

(23) Brown, J. M. *Chem. Soc. Rev.* **1993**, *22*, 25−41.

(24) Preliminary communication: Gridnev, I. D.; Higashi, N.; Imamoto, T. *J. Am. Chem. Soc.* **2000**, *122*, 10486-10487.

(25) Brufani, M.; Filocamo, L.; Lappa, S.; Maggi, A. *Drugs Future* **1997**, *22*, 397−410.

(26) Cutler, N. R.; Polinsky, R. J.; Sramek, J. J.; Rnz, A.; Jhee, S. S.; Mancione, L. *Acta Neurol. Scand.* **1998**, *97*, 244−250.
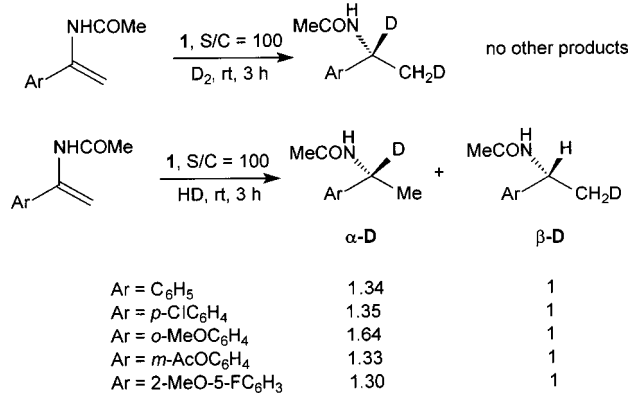
(27) Enz, A.; Boddeke, A. H.; Gmelin, G.; Malanowski, J. *Prog. Brain Res.* **1993**, *98*, 431−438.

(28) Ohara, T.; Tanaka, K.; Fukaya, H.; Demura, N.; Iimura, A.; Seno, N. *Behav. Brain Res.* **1997**, *83*, 229−233.
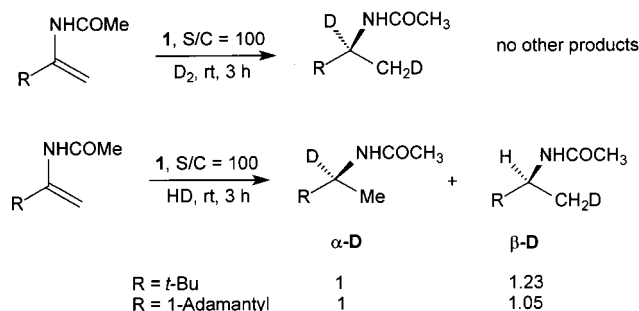
(29) Tse, F. L. S.; Laplanche, R. *Pharm. Res.* **1998**, *15*, 1614−1620.

(30) Burk, M. J.; Casy, G.; Johnson, N. B. *J. Org. Chem.* **1998**, *63*, 6084−6085.

Scheme 3

Ar	α-D	β-D
Ar = C$_6$H$_5$	1.34	1
Ar = p-ClC$_6$H$_4$	1.35	1
Ar = o-MeOC$_6$H$_4$	1.64	1
Ar = m-AcOC$_6$H$_4$	1.33	1
Ar = 2-MeO-5-FC$_6$H$_3$	1.30	1

Scheme 4

R	α-D	β-D
R = t-Bu	1	1.23
R = 1-Adamantyl	1	1.05

obtain further insight into the origin of this phenomenon, we undertook a mechanistic investigation of the asymmetric hydrogenation of enamides catalyzed by the Rh-BisP* catalyst.

Asymmetric Hydrogenation of Enamides Using D$_2$ and HD. The preceding research showed that the nature of the isotope partitioning in the products and intermediates of the catalytic asymmetric hydrogenation using deuterium hydride may provide valuable information on the reaction pathways and the structure of the intermediates.[14,17,31,32] On the other hand, by studying the catalytic deuteration the reversibility of the catalytic reaction can be checked as well as the possible intervention of the solvent in the catalytic cycle of the asymmetric hydrogenation.[14,31,32]

We studied the catalytic hydrogenations of a series of enamides using D$_2$ and HD. The complete absence of isotopic scrambling was found in all deuteration experiments; only the dideuteration products were observed (Schemes 3 and 4; errors in the isotopomeric excess determination did not exceed ±0.05). Usually, the same results were obtained when the deuteration was carried either in methanol or THF. Only in the case of o-methoxyphenyl-substituted enamide was a 10% admixture of the monodeuterated product (deuterium in the β-position) obtained in methanol. This result may be explained by the relatively slow reductive elimination resulting in the partial isotope exchange in the long-lived monohydride intermediate (see below). Thus, the deuteration experiments indicate that, once the hydrogen (or deuterium) atom is transferred in the migratory insertion step, the reaction does not reverse to free H$_2$.[31,32]

In the hydrogenation using HD an unequal distribution of deuterium between the α- and β-positions of the hydrogenation product was observed (Schemes 3 and 4). All aromatic enamides give predominantly the isomer containing deuterium at the

α-position (Scheme 3), in accordance with the previous results of similar experiments carried out with dehydroamino acids.[14,17,31,32] On the other hand, the reaction of t-Bu-substituted enamide **6** with HD gave a significant predominance of the β-deuterated product, whereas in the case of adamantyl-substituted enamide **7** almost equal quantities of α- and β-deuterated compounds were obtained (Scheme 4). Thus, the isotope partitioning in asymmetric hydrogenation with HD evidently correlated with the difference in the stereochemical outcome of the hydrogenation. We considered that the different reaction pathways may be responsible for these effects and studied the structure of the intermediates in the catalytic cycles of both aromatic and aliphatic enamides.

An additional interesting effect was noticed in these experiments. In most of the studied cases the enantiomeric excesses of the hydrogenation products from the experiments using HD and D$_2$ reproduced well the ee values obtained with dihydrogen. However, a significant decrease of the optical yield was observed in the case of o-methoxyphenyl-substituted enamide. Thus, the ee in the hydrogenation of this substrate with H$_2$ was 50% (Table 1, entry 3). In the hydrogenation with HD under the same conditions the ee was drastically decreased (24% ee in two independent runs). Use of D$_2$ led again to a drastic decrease of ee: 12% and 5% ee were obtained in two independent experiments. To our knowledge, this is the first observation of the significant dependence of the optical yield on the isotopic composition of the hydrogenation reagent. Most likely either kinetic or equilibrium isotope effects, or a combination of both, are responsible for such drastic change in the ee.

Intermediates in the Asymmetric Hydrogenation of Phenylenamide (5) and p-Clorophenylenamide (10). Addition of a 2-fold excess of enamides **5** or **10** to a deuteriomethanol solution of solvate complex **11**[17] at −20 °C resulted in immediate formation of two diastereomers of catalyst−substrate complexes **12** or **13** in a ratio changing from 4:1 at −90 °C to 2:1 at 0 °C (**12**, ΔH = −1.3 kcal mol^{-1}, ΔS = −3.0 cal mol^{-1} K^{-1}) or from 13:1 at −90 °C to 3:1 at 0 °C (**13**, ΔH = −1.5 kcal mol^{-1}, ΔS = −3.2 cal mol^{-1} K^{-1}) (Scheme 5). In both cases, no detectable amounts of the solvate complex **11** could be found in the spectra in the temperature range from −90 to +30 °C, and, therefore, the tightness of binding for these substrates (**5** and **10**) is comparable to that in the catalyst−substrate complex of **11** and methyl (Z)-α-acetaminocinnamate.[17] The spectral data for the catalyst−substrate complexes **12** and **13** are given in Tables S2−S4. All spectral properties of **12** and **13**, including the temperature dependence of the NMR spectra, are essentially similar; in the following section we describe in detail the spectral characteristics of **12**, making reference to the spectra of **13** only when necessary.

The configurations of major and minor isomers **12a** and **12b** were elucidated from the NMR data. A portion of the 2D ^{1}H−^{31}P correlation spectrum is shown in Figure 1. It reveals a remarkable difference in the chemical shifts of the alkyl groups of **12a** and **12b**. In the major isomer the difference in chemical shifts of two unequal t-Bu groups is 0.60 ppm, whereas the methyl groups are separated by only 0.18 ppm. The reverse situation is evident in the spectrum of **12b**: only a small difference (0.10 ppm) is observed for the signals of the t-Bu groups, but Δδ(Me) is as great as 1.05 ppm. Inspection of the molecular models of **12a** and **12b** shows that the observed differentiation in the chemical shifts can be explained by the shielding effect of the phenyl ring: In **12a** one of the t-Bu groups is shielded, and its chemical shift is, therefore, highfield shifted. In **12b** the same effect was observed for one of

(31) Brown, J. M.; Parker, D. *Organometallics* **1982**, *1*, 950−956.

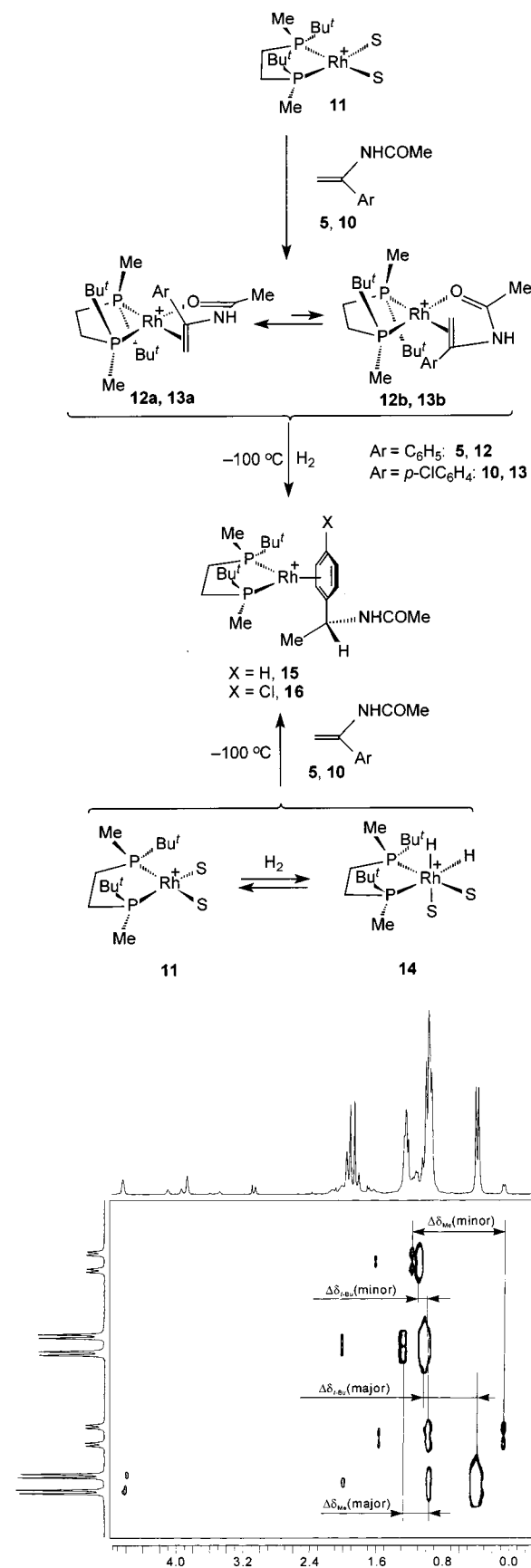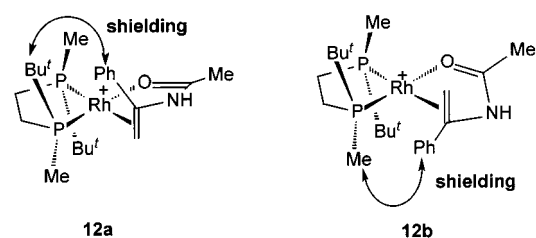(32) Brauch, T. W.; Landis, C. R. *Inorg. Chim. Acta* **1998**, *270*, 285−297.

Asymmetric Hydrogenation of Enamides

J. Am. Chem. Soc., Vol. 123, No. 22, 2001 5271

Scheme 5

Scheme 6

unexpected and demonstrates that the phenyl ring can minimize its steric demands by acquiring favorable conformation.

The structures of the major and minor isomers of **13** (see Tables S2–S4) were assigned on the basis of the same reasons; the major isomer **13a** has the structure similar to **12a**: the *p*-Cl-phenyl substituent in **13a** is close to one of the *t*-Bu groups, as follows from the analysis of the relative chemical shifts.

The ^{31}P NMR spectra of **12** are temperature-dependent. At temperatures below −40 °C the line shape of the ^{31}P NMR spectrum of **12** is unaffected by the dynamic effects, whereas at higher temperatures the reversible broadening of the spectral lines attests to the reversible interconversion of the diastereomers **12a** and **12b** (Figure S1). The mechanism of this interconversion was elucidated from the EXSY spectra. Figure 2 displays the phase-sensitive 2D ^{31}P–^{31}P EXSY spectra of the equilibrium mixture of **12a** and **12b** at two different temperatures. In the spectrum taken at −40 °C (Figure 2, left) only two cross-peaks corresponding to the pairwise exchange of P^1 and P^2 in two isomers are observed. This attests to the intramolecular exchange of **12a** and **12b** without complete dissociation of the substrate. On the other hand, in the EXSY spectrum taken at −25 °C, all possible cross-peaks between four signals are observed, although their intensity is different (Figure 2, right). The two most intensive cross-peaks are the same as those observed at −40 °C, and, therefore, the intramolecular exchange of **12a** and **12b** is still the fastest process at −25 °C. Four much less intensive cross-peaks indicate the occurrence of intermolecular exchange via complete dissociation of either **12a** or **12b** producing a free substrate and solvate complex **11**. In the ^{1}H–^{1}H EXSY spectrum taken at −30 °C a set of exchange cross-peaks between free enamide and coordinated enamide was observed, confirming the dissociation mechanism. Thus, two diastereomers **12a** and **12b** interconvert reversibly via intra- and intermolecular pathways. The interconversion via the intramolecular mechanism is notably faster at −25 °C. Similar equilibria were previously observed for various catalyst–substrate complexes of dehydroamino acids.[14,17,33–35]

It should be noted that the rate of intermolecular interconversion of **12a** and **12b** is significantly faster compared to that in the catalyst–substrate complexes of dehydroamino acids. The quantification of the EXSY data gives for the intermolecular interconversion of the diastereomers of **12** free activation energy $\Delta G_{248} = 14$ kcal mol^{-1}, which is approximately 5 kcal mol^{-1} lower compared to that for the complex of **11** and methyl (*Z*)-α-acetaminocinnamate.[17]

We attempted to detect a monohydride intermediate in the asymmetric hydrogenation of **5** catalyzed by **11**. However, either the addition of **5** to a deuteriomethanol solution of a dihydride complex **14**[17] at −100 °C or hydrogenation of **12** at −100 °C produced directly a catalyst–product complex **15** in equilibrium with solvate **11** (Scheme 5). The same result (producing complex **16**) was obtained when the catalyst–substrate complex **13** was hydrogenated at −100 °C. The optical yields of the hydrogenation products obtained in the NMR experiments were always the same as those in the catalytic hydrogenation.
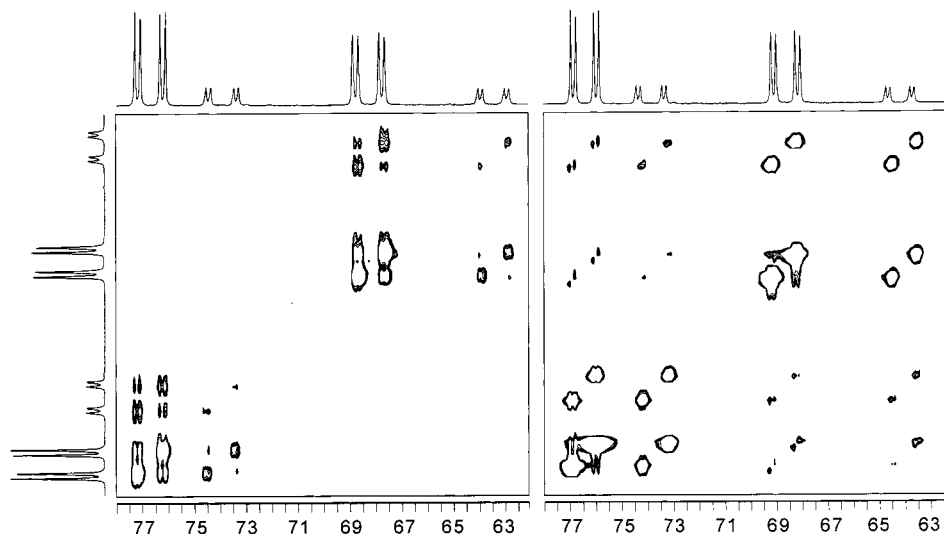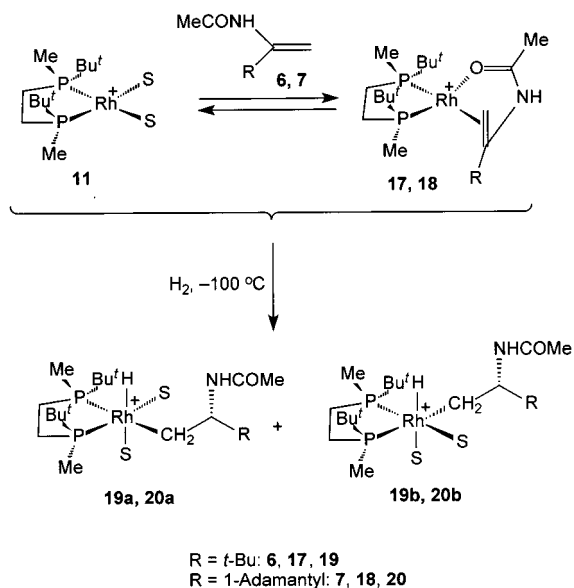
Figure 1. ^{1}H–^{31}P HMBC spectrum of **12** (400 MHz, −20 °C, CD$_3$-OD).

the methyl groups. We conclude, therefore, that the major isomer of **12** has the structure **12a** (Scheme 6). This is somewhat

Figure 2. $^{31}P-^{31}P$ EXSY spectra of **12** (162 MHz, CD$_3$OD): (left) at 223 K, mixing time 1 s; (right) at −25 °C, mixing time 0.1 s.

Scheme 7

R = *t*-Bu: **6**, **17**, **19**
R = 1-Adamantyl: **7**, **18**, **20**

| Abs energy, au: | −922.360301541 | −922.360841652 |
| Rel energy, kcal mol^{-1}: | 0.34 | 0 |

Figure 3. DFT-optimized structures (B3LYP/LANL2DZ) of **17′a** and **17′b**.

Intermediates in the Asymmetric Hydrogenation of *tert*-Butylenamide (6) and 1-Adamantylenamide (7). Addition of a 2-fold excess of *t*-Bu-substituted enamide **6** or adamantyl-substituted enamide **7** to the deuteriomethanol solution of solvate complex **11** resulted in formation of the catalyst−substrate complexes **17** and **18**, respectively, which differ significantly from **12** and **13** in structure and stability (Scheme 7).

The temperature dependencies of the ^{31}P NMR spectra of **17** and **18** (e.g. Figure S2) show that significant amounts of **11** equilibrate with the excess of either **17** or **18** even at −90 °C. The thermodynamic parameters of these are $\Delta H = -2.1$ kcal mol^{-1}, $\Delta S = -3.9$ cal mol^{-1} K^{-1} (**17**) and $\Delta H = -2.4$ kcal mol^{-1}, $\Delta S = -3.3$ cal mol^{-1} K^{-1} (**18**). In both cases only one isomer of the corresponding catalyst−substrate complex was observed in the temperature range from −90 to +30 °C; neither the line shape of the 1D NMR spectra nor 2D EXSY experiments carried out at various temperatures showed the presence of the second possible diastereomer. The relatively weak coordination of enamides **6** and **7** in the catalyst−substrate complexes **17** and **18** manifests itself also in the chemical shifts of the coordinated double bonds in their ^{13}C NMR spectra. Thus, the difference in chemical shifts of the coordinated double bond
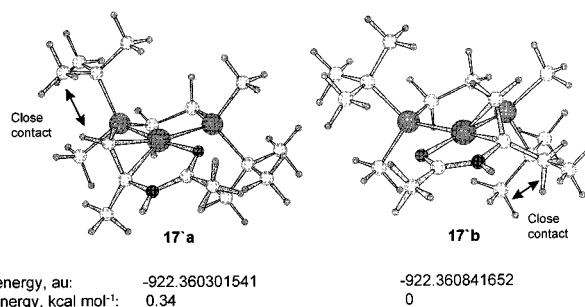
in **17** and the noncoordinated one in **6** is only 27 (for the CH$_2$ group) and 13 (for C$_{tert}$) ppm (27 and 9 ppm, respectively, in the case of **18**); the corresponding differences are 44 and 48 ppm in **12**. These values suggest also that, in contrast to **12** and **13**, the double bond is weakly coordinated in **17** and **18**. This conclusion seems to be reasonable in view of the bulkiness of the *t*-Bu and 1-adamantyl substituents.

In the phase-sensitive $^{31}P-^{31}P$ EXSY spectra of **17**, the exchange cross-peaks were observed between the doublet of **11** and each of the multiplets of **17**, as well as between the multiplets of **17**. Very similar results were observed in the EXSY spectra of the catalyst−substrate complex **18**.

We failed to determine experimentally the configurations of **17** and **18**: all alkyl groups resonate very closely in the ^1H NMR spectra of these catalyst−substrate complexes, retarding the chemical shift assignment. We therefore decided to resolve this problem computationally. DFT calculations of simplified molecules **17′a** and **17′b** gave virtually equal energies for these isomers: the energy difference is less than 0.5 kcal mol^{-1} (Figure 3). Nevertheless, the computed structures of **17′a** and **17′b** (Figure 3) give some indication of the possible reasons for the different stability of the real compounds. Analyzing the structures of **17′a** and **17′b**, one can see two competing effects influencing the stability of a certain isomer. The terminal CH$_2$= group in **17′a** is disposed almost in the plane of the chelate cycle of the catalyst, thus avoiding close contact with the bulky *t*-Bu substituent. On the other hand, in **17′b** this close contact is avoided at the expense of placing the methyl substituent of the substrate in close proximity to the *t*-Bu group from the catalyst (Figure 3). It is clear that the exact nature of the substituent in the α-position of enamide would determine the

Table 2. Parameters of the ^{1}H and ^{31}P NMR Spectra of the Monohydride Intermediates **19a,b**, **20a,b**, and **23a–c**

compd	δH ($^1J_{RhH}$, $^2J_{PH}$)	δ^{31}P^1 ($^1J_{RhP}$)	δ^{31}P^2 ($^1J_{RhP}$)
19a	−21.2 (26, 17, 31)	53.2 (86)	86.7 (162)
19b	−23.1 (32, 15, 32)	45.6 (82)	77.6 (152)
20a	−21.3 (27, 16, 27)	53.4 (86)	86.7 (160)
20b	−23.5^a	45.7 (86)	77.6 (150)
23a	−24.7 (39, 17, 28)	54.9 (81)	71.2 (133)
23b	−21.5 (28, 14, 28)	53.4 (89)	87.8 (160)
23c	−23.2 (32, 16, 32)	45.8 (83)	78.7^a

^{a} Couplings were not determined due to the very low concentration or overlapping with other signals.

relative stabilities of the diastereomers. Our experimental data show that in the case of flat aryl substituents, the steric repulsion from the *t*-Bu group can be minimized by acquiring an appropriate conformation, and the major diastereomers **12a** and **13a** have structures similar to **17′b**. Apparently, in the case of *t*-Bu- and 1-adamantyl-substituted substrates the steric repulsion from the bulky alkyl groups becomes more important than that from the terminal CH$_2$ group, and only **17a** and **18a** are observed experimentally in solution. Recently, very similar computational results for a complex of the Rh-DuPHOS catalyst and a model substrate were reported.[34]

Hydrogenation of the equilibrium mixture of **11**, **6**, and **17** (or **11**, **7**, and **18**) at −100 °C for 7 min followed by immediate placement of the sample in the probe of an NMR spectrometer precooled to −100 °C led to the observation of the monohydride intermediates **19** and **20** (Scheme 7). In both cases two isomers were observed in a 10:1 ratio. Monohydrides **19** and **20** are relatively stable below −85 °C; at higher temperatures they decompose rapidly, affording **11** and the corresponding hydrogenation products. The optical yields and the sense of stereoselection of the hydrogenation products obtained in the NMR experiments were always the same as in the catalytic hydrogenations (99% ee *S*). The spectral characteristics of **19** and **20** are very similar (Table 2).

In the ^{1}H NMR spectrum of **19** the hydride proton resonates at $\delta = -21.2$ as an 8-line multiplet (coupling with Rh is 28 Hz; that with phosphorus is 16 and 28 Hz). These values are close to the NMR spectra of the previously characterized monohydride intermediates in the asymmetric hydrogenation of dehydroamino acids.[14,17,35,36] However, the ^{31}P NMR spectrum displays significant difference. Thus, in all monohydride intermediates characterized previously, both phosphorus atoms resonate quite near, within the 15 ppm interval. On the other hand, in **19a** the difference in chemical shifts of two phosphorus atoms is more than 30 ppm ($\delta(P^1) = 51.9$, $\delta(P^2) = 85.3$) (Figure 4a). The chemical shift of the low-field signal is very close to that in the solvate complex **11** ($\delta = 89.8$). Therefore, the larger value of $\delta(P^2)$ in **19a** suggests that the coordination site disposed trans to this phosphorus atom is occupied by a weakly bound molecule of the solvent, and the carbonyl group is, accordingly, not coordinated. The same conclusion follows from the analysis of the carbonyl region of the ^{13}C NMR spectrum of **19a**. Thus, the signal of the carbonyl carbon of **19a** ($\delta = 176.3$) is only slightly downfield-shifted respective to the carbonyl signals of the starting enamide **6** ($\delta = 173.1$) and the hydrogenation
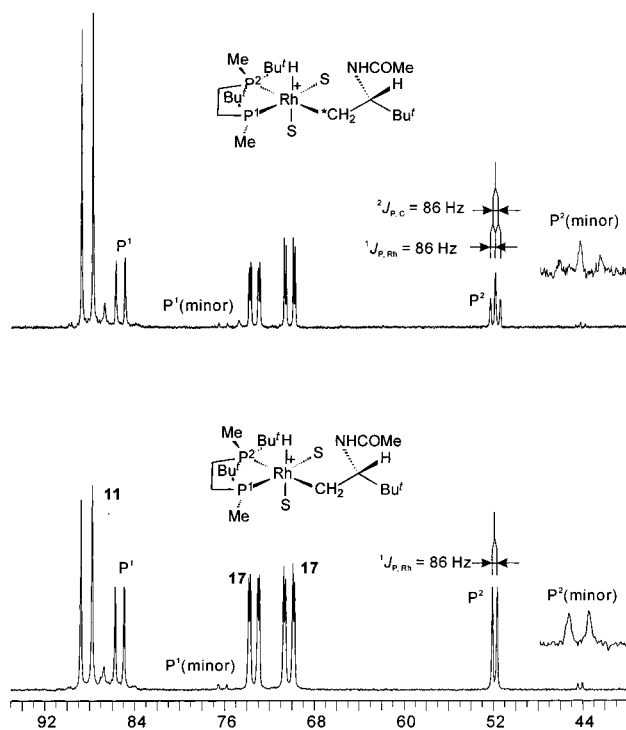
(33) Bircher, H.; Bender, B. R.; Philipsborn, W. v. *Magn. Reson. Chem.* **1993**, *31*, 293–298.

(34) Landis, C. R.; Feldgus, S. *Angew. Chem., Int. Ed.* **2000**, *39*, 2863–2866.

(35) Brown, J. M.; Chaloner, P. A. *J. Chem. Soc., Perkin Trans. 2* **1987**, 1583–1588.

(36) Landis, C. R.; Halpern, J. *J. Am. Chem. Soc.* **1987**, *109*, 1746–1754.

Figure 4. ^{31}P NMR spectra (162 MHz, −90 °C, CD$_3$OD) of the reaction mixtures containing monohydride intermediates: (a) **19** and (b) **19***.

Scheme 8
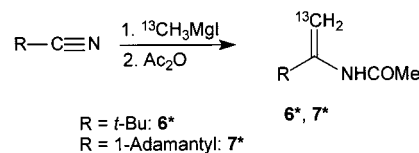
product ($\delta = 172.5$). Note also that the signal of the coordinated carbonyl of the catalyst−substrate complex **17** resonates at $\delta = 185.0$ and is split in a doublet with 7 Hz coupling. Additional information on the structure of the monohydride intermediate **19a** gives a broadened signal at 61.7 ppm in the ^{13}C NMR spectrum. This value of chemical shift corresponds to the carbon atom attached to the nitrogen. In the gated-decoupled experiment this signal becomes a doublet, and, therefore, it belongs to a methyne carbon. These data lead to the conclusion that the monohydride intermediate of the asymmetric hydrogenation of enamide **6** has the structure in which the amide is bound to Rh by the CH$_2$ group, and the α-position is hydrogenated.

It was very difficult to locate the signal of the CH$_2$Rh carbon in the ^{13}C NMR spectrum due to its relatively low intensity and partial overlap with other much more intensive signals. To obtain unequivocal confirmation of the structure of monohydrides **19** and **20**, we prepared β-labeled compounds **6*** and **7*** (Scheme 8) and carried out the hydrogenation experiments under the same conditions as for the unlabeled compounds.

Figure 4b shows the ^{31}P NMR spectrum containing the signals of the labeled monohydride intermediate **19***. The evident difference from the spectrum of the unlabeled compound (Figure 4a) is the multiplicity of the high-field signal: in the spectrum of the labeled compound it resonates as a double doublet with two equal couplings (86 Hz). One of these couplings is $^1J_{Rh−P}$, and the other one is undoubtedly $^2J_{C,−P}$, since it is absent in the spectrum of the unlabeled compound. The presence of a large coupling $^2J_{C−P}$ with the *trans*-phosphorus atom in the ^{31}P NMR spectrum of **19*a** unequivocally proves the proposed structure
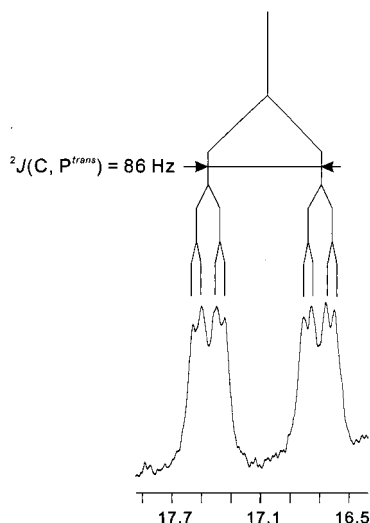
Figure 5. Multiplet of the CH$_2$Rh group in the ^{13}C NMR spectrum of **19*** (125 MHz, −90 °C, CD$_3$OD).

of the monohydride intermediate. The multiplet of the CH$_2$Rh group of **19*a** (Figure 5) resonates at $\delta = 15.8$ and displays the characteristic couplings $^2J_{C-P} = 86.5$ Hz and $^1J_{Rh-C} = 20$ Hz. It is noteworthy that the signal of the high-field phosphorus of minor isomer **19*b** in the ^{31}P NMR spectrum is also split in a triplet (Figure 4b). This allows assignment of its structure as the Rh-diastereomer of **19*a** (as shown in Scheme 7), since the observed enantioselectivity is higher than that calculated based on the relative amounts of **19a** and **19b**, and the minor isomer cannot, therefore, have an alternative configuration at the α-carbon.

Intermediates in the Asymmetric Hydrogenation of *o*-Methoxyphenylenamide (21). In all the previous examples we studied, the intermediates of the catalytic reactions gave very high optical yields. However, in certain cases much lower optical yields were obtained in catalytic hydrogenation (entries 3 and 9 in Table 1). We chose to study the reaction pathway for the hydrogenation of *o*-methoxyphenyl-substituted enamide **21** to determine the correlation of the structure and stability of the observed intermediates with the relatively low enantioselectivity observed in this case.

The catalyst−substrate complex **22** obtained by addition of a 2-fold excess of enamide **21** to the deuteriomethanol solution of the solvate complex **11** exists in solution as a mixture of two interconverting diastereomers **22a** and **22b**. The ratio **22a**: **22b** changes from 15:1 at −90 °C to 6:1 at 0 °C (thermodynamic parameters of the equilibrium could not be determined accurately in this case due to the presence of small amounts of **11** and an additional unidentified complex in equilibrium with **22a,b** and **11**, detectable in the temperature interval from −90 to −60 °C). A small amount of **11** equilibrates with **22** even at −90 °C. The configuration of the main isomer **22a** is the same as that of **12a** and **13a**; in this case $\Delta\delta Bu^t$,major = 0.89, $\Delta\delta$Me,major = 0.15 and $\Delta\delta Bu^t$,minor = 0.20, $\Delta\delta$Me,minor = 1.05.

Hydrogenation of the equilibrium mixture of **11**, **21**, and **22** carried out at −100 °C resulted in the detection of three isomers of monohydride intermediate **23a−c** in 100:34:10 ratio (Figure 6). The structures of **23a−c** were determined by using the NMR data (Table 2). In the hydride region of the ^{1}H NMR spectrum taken at −90 °C (Figure 6a) three hydride signals were found. Heteronucleus correlation experiments and selective ^{31}P decouplings made possible the assignments in the ^{31}P NMR spectrum. The NMR spectra of the monohydrides **23b,c** are similar to those of **19** and **20** (Table 2). They also have similar thermal stability
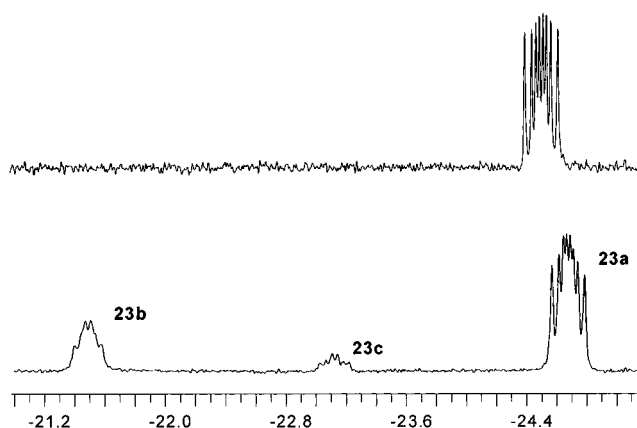

Figure 6. Hydride region of the ^{1}H NMR spectrum of **23** (400 MHz, CD$_3$OD): (a) at −90 °C and (b) at −50 °C.
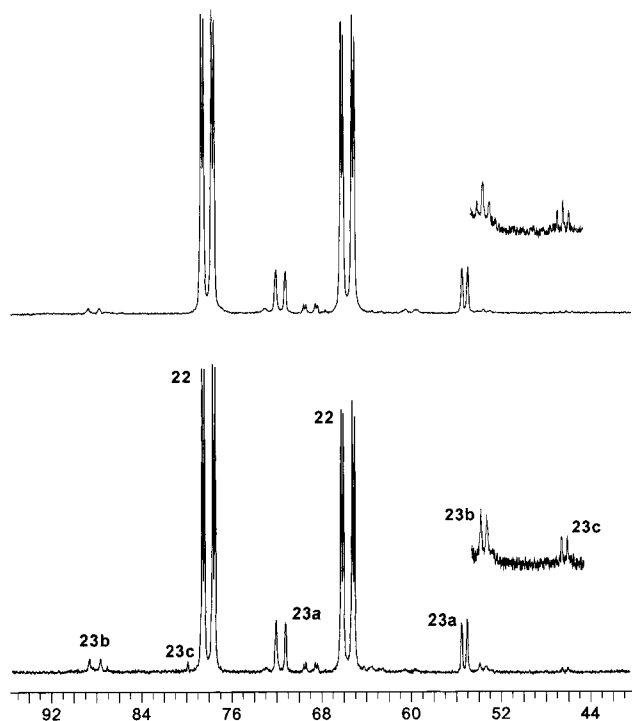

Figure 7. ^{31}P NMR spectra (162 MHz, −95 °C, CD$_3$OD) of the reaction mixtures containing monohydride intermediates: (a) **23a−c** and (b) **23a−c***.

and decompose rapidly if the temperature of the sample is raised over −85 °C. On the other hand, the hydride signal of **23a** in the ^{1}H NMR spectrum is significantly high-field shifted and has an unusually large value of $^1J_{Rh-H}$ (39 Hz). In addition, the coupling $^1J_{Rh-P}$ of the low-field phosphorus is about 20% smaller in value compared to the same couplings in **23b,c** and is almost equal to the couplings in the previously characterized monohydride intermediates with the α-C atom bound to rhodium.[14,17,37,38] Conclusive evidence of the structures of **23a−c** was obtained in the hydrogenation experiment using a ^{13}C-labeled enamide **21*** prepared similarly to the labeled compounds **6** and **7** (Scheme 8). The ^{31}P NMR spectra of the samples containing labeled and unlabeled compounds are compared in Figure 7. The signals of the major monohydride species **23a** remained unchanged: no significant coupling with

(37) Chan, A. S. C.; Halpern, J. *J. Am. Chem. Soc.* **1980**, *102*, 838−840.

(38) Brown, J. M.; Chaloner, P. A. *J. Chem. Soc., Chem. Commun.* **1980**, 344−346.

**Scheme 9**

Ar = 2-MeOC$_6$H$_4$

Scheme 10
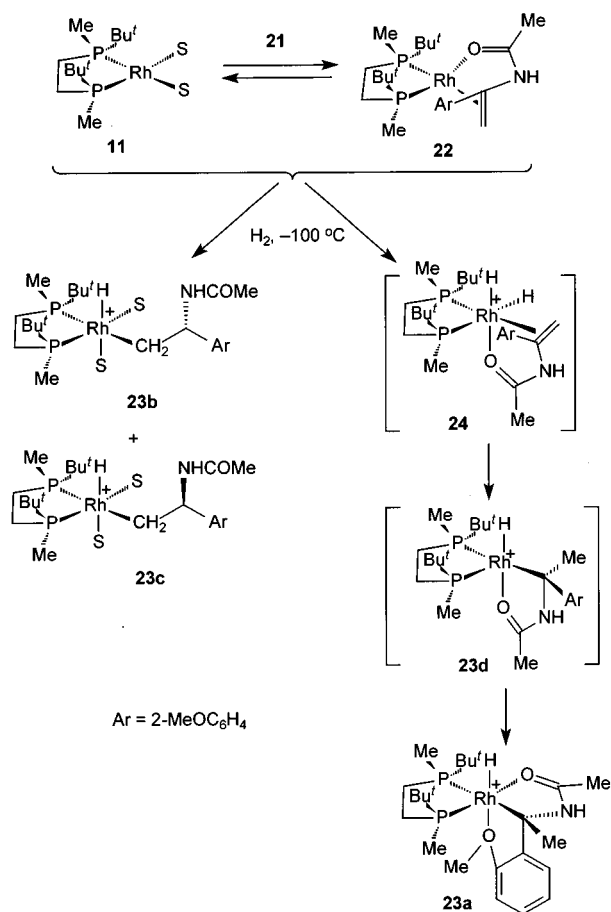
the ^{13}C nucleus is observed. This means that in **23a** the rhodium atom is bound to the quaternary carbon atom, and the labeled carbon should appear as a signal of the methyl group uncoupled to phosphorus and rhodium, which indeed was found at $\delta =$ 31.8 in the ^{13}C NMR spectrum. On the other hand, the high-field signals in the ^{31}P spectrum belonging to **23b*** and **23c*** are split in triplets, attesting to the presence of the *CH$_2$–Rh bonds in these intermediates, and supporting the structures drawn in the Scheme 9 (see the above discussion for **6*** and **7***).

The monohydrides **23b** and **23c** can have different configuration either on carbon or on rhodium. These two possibilities cannot be distinguished from their NMR spectra. Nevertheless, comparing the relative integral intensities in the ^{1}H NMR spectrum of the mixture of dihydrides and the experimental ee obtained after quenching the NMR sample, a definite conclusion can be made on the structure of **23b** and **23c**. Indeed, the ratio ([**23a**] + [**23c**] − [**23b**]):([**23a**] + [**23b**] + [**23c**]) (0.53) corresponds exactly to the ee of the hydrogenation product obtained after quenching of this sample (53%) and is close to the ee value obtained under catalytic conditions (50%). Since the deuteration experiments attest to the irreversibility of the migratory insertion step, we conclude that **23a** and **23c** produce *R*-amide, whereas **23b** is a precursor of *S*-amide. Therefore, the configurations of the α-carbon atoms are different in the diastereomeric monohydrides **23b** and **23c**.

The relative stability of the monohydride intermediate **23a**, compared to monohydrides from the catalytic cycles of the hydrogenation of **5** and **10**, apparently results from the possibility of its stabilization with the adjacent *o*-methoxy group (Scheme 9). Thus, our attempt to detect a monohydride from *p*-methoxy-substituted enamide, which apparently has similar
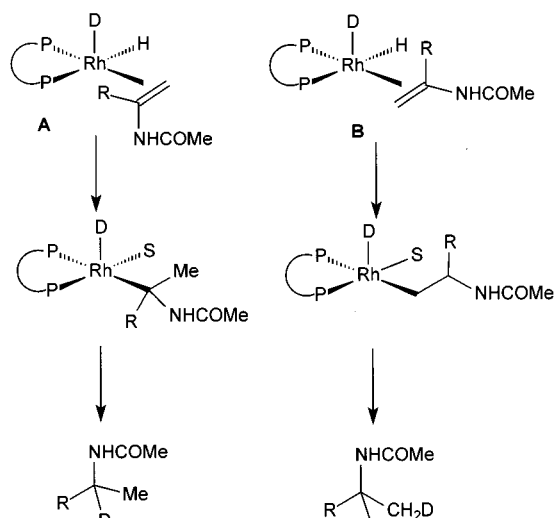
electronic properties with **21**, was unsuccessful: the hydrogenation of the corresponding catalyst−substrate complex at −100 °C gave directly the hydrogenation product. Similar stabilization through terdentate coordination has been reported for structurally similar Rh[17] and Ru.[39] However, the monohydride intermediate **23a** cannot form directly from its likely precursor, dihydride intermediate **24**, since the vacant coordination site after the migratory insertion is naturally placed in the trans-position relative to the *o*-methoxyphenyl substituent (Scheme 9). Apparently, the initially formed monohydride intermediate **23d** undergoes fast rearrangement to **23a** via a simple rotation around the Rh−C bond.

Mechanism of Stereoselection in the Catalytic Asymmetric Hydrogenation of Enamides. The outcome of the experiments using HD corresponds well to the structures of the observed monohydride intermediates. Upon hydrogenation of solvate **11** with HD, the isotopomer of **14^d** with apical disposition of deuterium forms predominantly with the factor 1.3($\pm$0.1):1.[17] On the other hand, the equatorial hydride is transferred in the migratory insertion step. If the consequence of substrate coordination and migratory insertion is faster than the interconversion of isotopomers, the partitioning of deuterium in the products indicates the fashion of the substrate coordination during the migratory insertion step. Therefore, the predominance of the α-deuterated product corresponds to coordination of type **A** (Scheme 10) and subsequent formation of a monohydride intermediate with the tertiary carbon atom bound to rhodium, whereas the predominance of the β-deuterated product implies the coordination of type **B** and a monohydride intermediate with the CH$_2$ group bound to the rhodium atom.

The observation of the monohydride intermediates **19** and **20** with the β-carbon atom attached to Rh is in accord with the deuterium partitioning in the products of hydrogenation of enamides **6** and **7** with HD. The opposite sense of deuterium partitioning in the reactions using aromatic enamides implies another pathway through **A**-type coordination (Scheme 10).

There are four different ways for coordination in each of the pathways **A** and **B**. However, we rule out the possibility of coordination of the double bond of an enamide to the apical coordination site of rhodium due to the evident steric hindrance to such coordination arising from the alkyl substituents of the catalyst. The remaining four isomers of a hypothetical dihydride

(39) Wiles, J. A.; Bergens, S. H.; Young, V. G. *J. Am. Chem. Soc.* **1997**, *119*, 2940−2941.

Scheme 11

A1   A2

B1   B2
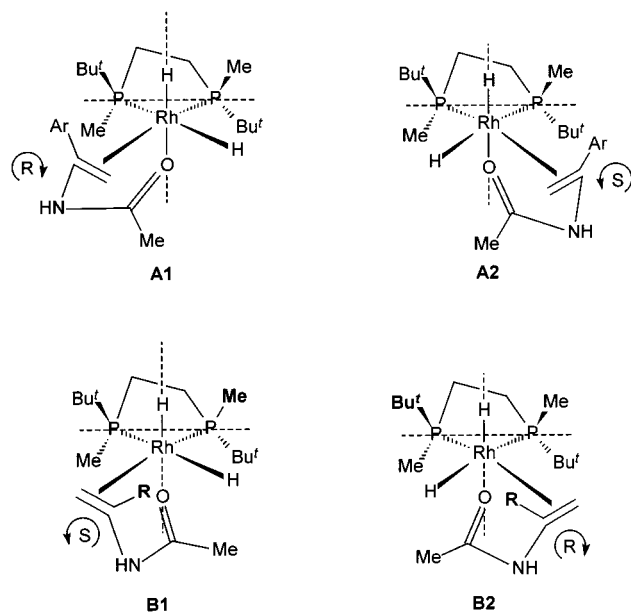
intermediate are shown in Scheme 11. Similarly to the asymmetric hydrogenation of dehydroamino acids,[17] we conclude that the main stereoregulating factor in the case of pathway **A** is the steric interaction between the chelate ring made by the substrate and the adjacent alkyl group of the catalyst. In the dihydride intermediate **A1** this interaction is effectively reduced (the chelate ring is close to the Me group of the catalyst), which is in accord with *R*-stereoselection observed in the hydrogenation of aromatic enamides.

In the case of the enamides containing bulky *t*-Bu and adamantyl substituents, intermediate **A1** becomes less accessible: reducing the steric repulsion between the chelate cycle of the substrate and the alkyl groups of the catalyst automatically leads to drastic hindrance between the *t*-Bu group of the catalyst and the *t*-Bu or adamantyl group of the substrate, and vice versa, if the latter interaction is avoided in intermediate **A2**, the close contact of the chelate cycle and the *t*-Bu group of the catalyst increases the energy of this configuration.

Therefore, it is reasonable to conclude that bulky enamides choose an alternative mode of coordination, in which the substituent of the substrate is much farther distanced from the alkyl groups of the catalyst (intermediates **B1** and **B2** in Scheme 11). The relative availability of these intermediates is now determined by the remaining interaction between the bulky group R (*t*-Bu or adamantyl) and one of the alkyl groups of the catalyst: a methyl group in the case of **B1** and a *t*-Bu group in the case of **B2**.

In the case of the *o*-methoxyphenyl-substituted enamide **21**, these two reaction pathways are apparently competitive. Since the ratio of the observed monohydride intermediates **23a−c** is equal to the ee observed in the catalytic hydrogenation, we may conclude that other competitive pathways do not contribute significantly to the flux of catalysis. This, in turn, leads to a conclusion that the intermediate formation of dihydride **A2** is less favored in this case than the intermediacy of **B1** or **B2**.

Conclusions

The *t*-Bu-BisP*-Rh catalyst is one of the best catalysts for the asymmetric hydrogenation of enamides reported so far. Various aryl-substituted enamides give the corresponding optically active amides with 96−99% ee, with the exception of ortho-substituted compounds which afford moderate enantioselectivity. Enamides containing *t*-Bu and 1-adamantyl groups at the α-position give excellent ee values, but the configuration of the hydrogenation products obtained with the use of the same catalyst is opposite to that of aryl-substituted enamides. This dramatic difference is explained by the opposite mechanisms of stereoselection operating in these polar cases. The relatively low optical yields observed for the *o*-methoxyphenyl- and *o*-chlorophenyl-substituted enamides may be attributed to the simultaneous running of both reaction pathways.

Supporting Information Available: Experimental details, Tables S1−S4, Figures S1 and S2, charts of NMR spectra for all important products and intermediates, and Cartesian coordinates for **17′a** and **17′b** (PDF). This material is available free of charge via the Internet at http://pubs.acs.org.

JA010161I